Optical Wireless OFDM System on FPGA: Study of LED Nonlinearity Effects

Irina Stefan*, Hany Elgala*, Raed Mesleh†, Dominic O'Brien‡ and Harald Haas*§
*Jacobs University Bremen, Campus Ring 1, 28759 Bremen, Germany, Email: i.stefan & h.elgala@jacobs-university.de
†University of Tabuk, Electrical Engineering Department, Tabuk, Saudi Arabia, Email: raed.mesleh@ieee.org
‡Department of Engineering Science, University of Oxford, Parks Road, Oxford OX1 3PJ, UK, Email: dominic.obrien@eng.ox.ac.uk
§Institute for Digital Communications, The University of Edinburgh, Edinburgh EH9 3JL, UK, Email: h.haas@ed.ac.uk

***Abstract*—Nonlinearities can drastically degrade the performance of OFDM (orthogonal frequency division multiplexing) based optical wireless (OW) communication systems using intensity modulation (IM) of the optical carrier. The light emitting diode (LED) transfer function distorts the signal amplitude and forces the lower signal peaks to be clipped at the LED turn-on voltage (TOV). Additionally, the upper signal peaks can result in optical output degradation. The induced distortion can be controlled by optimizing the bias point (BP) of the LED and/or backing-off the signal power modulating the LED. In this paper, the obtained experimental results using a hardware demonstrator for OW OFDM transmission based on field-programmable gate array (FPGA) and off-the-shelf analog components are presented. The conducted measurements for the bit-error performance focus on determining the optimum BP and optimizing the OFDM signal amplitude to obtain best performance. In this context, the experimental bit-error ratio (BER) is obtained as a function of the LED BP and the RMS (root mean square) OFDM signal across the LED.**

***Index Terms*—Optical wireless communication, OFDM, Nonlinearity, LED.**

I. Introduction

The requirements of low energy consumption and high speed transmission are well recognized in current and future mobile communication infrastructures. In this context, OW technology is emerging as a viable alternative to radio frequency (RF) technology. Recently, OFDM is considered by many researchers as a promising modulation scheme to increase the capacity of short-range indoor OW transmission [1–3]. This can be easily achieved by using high order multi-level quadrature amplitude modulation (M-QAM), where M is the number of discrete constellation points [4].

Communication systems, in general, suffer from the nonlinearity that is introduced by electronic components. When the OFDM signal with its envelope variations passes through a nonlinear device, in particular the power amplifier (PA) of an RF transmitter or the LED of an optical transmitter, it causes significant out-of-band radiation. This leads to a reduction in spectral efficiency and in-band distortion, which creates inter-carrier interference (ICI) and degrades the error performance [5].

In optical wireless systems, the LED is one of the main devices causing nonlinearity [6, 7]. As shown in Fig. 1, each LED has a minimum threshold value known as the TOV which is the onset of current flow and light emission (below the TOV, the LED is considered in a cut-off region and is not conducting current) [8]. Above the TOV, the current flow and light output increase exponentially with voltage (current conduction region). The LED emits light that is linear with the drive current. However, thermal aspects causing a drop in the electrical-to-optical conversion efficiency must be considered [8]. The DC and AC/pulsed currents must be adjusted to ensure that the LED chip does not overheat, in order to avoid degradation in output light or total failure in the worst case. These current values depend very much on the diode type and vary depending on the semiconductor materials, packaging, and ambient temperature. The aim of this study is to investigate via a hardware demonstrator the performance of optical OFDM systems in the presence of LED nonlinearity.

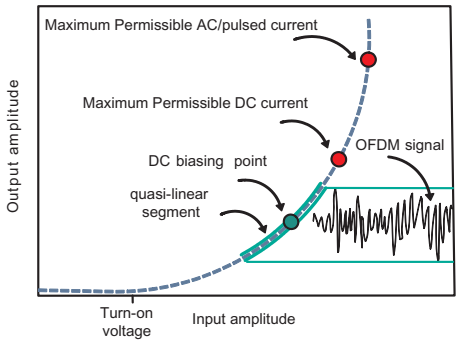

Fig. 1: Non-linear LED transfer characteristics: The typical relation between the applied forward voltage and the forward current through the LED is depicted. The nonlinear transfer characteristic distorts the OFDM signal.

The paper is organized as follows. Section II describes in details the optical OFDM model and its parameters. Section III gives the outline of the experimental setup. Relevant hardware properties are addressed in Section IV. The effective signal-to-noise ratio (SNR) which is used to explain the behavior of the obtained experimental curves is defined in Section V. Finally, performance results for uncoded 4-QAM OFDM transmission are shown in Section VI, followed by conclusions in Section VII.

II. OFDM system model

In OW, the real valued baseband OFDM signal is used to modulate the instantaneous power of the optical carrier resulting in IM. There are several forms of optical OFDM

978-1-4244-8331-0/11/$26.00 ©2011 IEEE

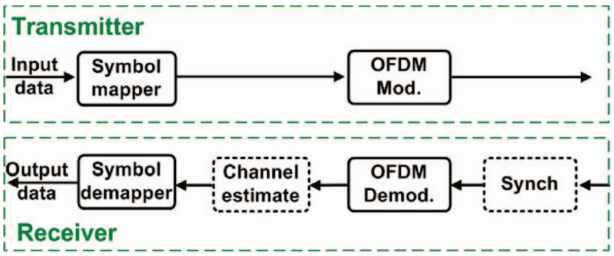

Fig. 2: The physical layer building blocks.

using IM. In this paper, the DC-biased OFDM (DCO-OFDM) is considered [2, 9, 10]. In DCO-OFDM, the bipolar time domain signal is used to modulate the LED. The physical layer (PHY) specifications are based on the worldwide interoperability for microwave access (WiMAX) standard, but with the necessary adaptations related to the specific nature of optical transmission, *e.g.* the requirement of a real valued OFDM signal.

The transmitter consists of symbol mapping, and OFDM modulation as shown in Fig. 2(a). The serial stream of data and the redundancy bits, such as the pilots symbols used for channel estimation and the Barker code used for frame synchronization are mapped into parallel streams through the symbol mapper. The OFDM modulation consists of 1) bit to symbol mapping operation 2) inverse fast Fourier transform (IFFT) operation, and 3) cyclic prefix (CP) addition. After being modulated, each symbols stream is transmitted on a separate subcarrier. The IFFT operation modulates and multiplexes the subcarriers. The baseband signal available after the IFFT operation needs to be real valued [10]. This is a major difference between optical and RF transmission based on OFDM. A real valued baseband signal can be easily obtained by using Hermitian transpose data symbols at the IFFT input, *e.g.* $X_n = X^*_{N-n}$, where $X_n, n = 0, \cdots, N-1$ are the input data symbols and N is the number of subcarriers. After generating a real time-domain OFDM symbol, a CP is added as a guard interval to avoid multipath induced inter-symbol interference (ISI). At the receiver, frame synchronization, channel estimation, and symbol equalization are realized using Barker codes and block-type pilots. Barker codes are subsets of pseudonoise (PN) sequences and are commonly used for frame synchronization in digital communication systems [11]. After the CP removal, the OFDM signal is converted back to the frequency domain by applying the fast Fourier transform (FFT) operation. Using the block-type pilots symbol, the channel is estimated in the frequency domain. The channel is assumed to remain static over one OFDM frame, so that once the channel is estimated, frequency domain equalization is realized to detect the original data bits using a conventional OFDM zero-forcing (ZF) equalizer.

The structure of an OFDM frame is presented in Fig. 3 with an enlarged view of the Barker code, pilot signal, and data symbols.

[1]The reader is kindly asked to refer to [4] for detailed information about optical OFDM

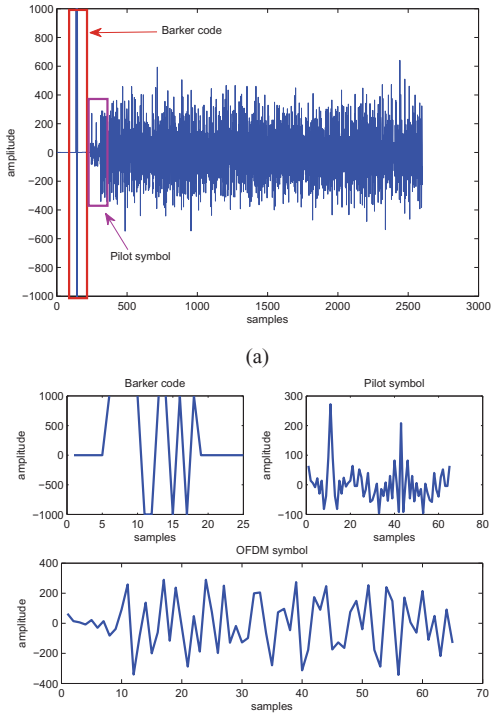

Fig. 3: (a) OFDM frame consisting of one synchronization symbol carrying the Barker code, one channel estimation block-type symbol, and 31 data symbols. (b) Enlarged view for the different symbol types.

III. Experimental Setup

The experimental setup for conducting measurements is shown in Fig. 4. The analog part includes the LED driver circuits and a photoreceiver module (see details in section IV). The digital signal processing (DSP) includes algorithms to generate and decode the optical OFDM signal and to interface with a computer.

The DSP is realized using a programmable logic device, *i.e.* FPGA. The DSP Development Kit, Stratix II Edition offers two 12-bit, 125 Msps analog-to-digital converters (Analog Devices AD9433) and two 14-bit, 165 Msps digital-to-analog converters (Texas Instruments Incorporated DAC904) [12].

IV. Analog Frontends

A. Transmitter module

In this study, a high-power IR LED from Hewlett Packard (HSDL-4220) is considered. This LED utilizes an Aluminum Gallium Arsenide (AlGaAs) chip and is packaged in clear 5 mm package. It is optimized for speed and efficiency at a peak emission wavelength of 875 nm. The DC forward current is 100 mA@1.5 V and the maximum allowed forward current, peak forward current (AC/pulsed current), is 500 mA@2.5 V. The TOV is considered at 1 mA which corresponds to a 1.3 V drop across the LED. This is the minimum allowed forward current according to the data sheet. At 100 mA DC forward current, the radiant optical power is typically 38 mW. The LED

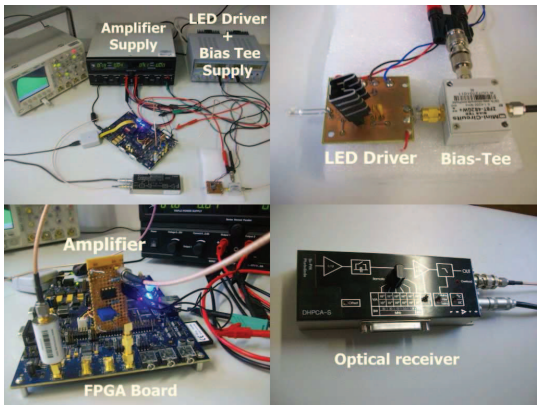

Fig. 4: The experimental setup to demonstrate a simplex IR transmission. It consists of a single FPGA development board from Altera, a single computer to configure the on-board FPGA chip, and analog optical front ends.

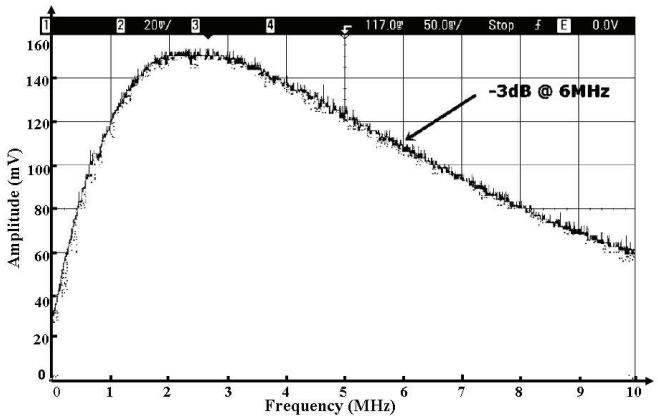

Fig. 5: The overall frequency response measured after the analog optical receiver module. The frequency sweep starts at 100 kHz and ends at 10 MHz.

has a 30 degree viewing angle and offers 9 MHz modulation bandwidth at 50 mA.

The LED driver is based on a pre-amplifier, a bias-tee, power supply, and a buffer amplifier. The pre-amplifier provides a voltage amplification to the time domain OFDM signal available after the on-board DAC. By aid of a bias tee, the amplified OFDM signal is superimposed onto the DC bias voltage (LED operational point). A buffer amplifier is used between the LED and the bias-tee to provide electrical impedance transformation to match the low impedance of the LED.

B. Receiver module

The receiver module is based on a Silicon PIN photodiode (PD) with a daylight filter. The active area is 2.2 mm x 2.2 mm. This PD offers 0.63 A/W absolute responsivity at 870 nm (maximum responsivity is at 900 nm). The dark current is typically 2 nA. After a transimpedance amplifier (TIA) configuration, the signal passes through AC/DC coupling, programmable gain amplifier, buffer amplifier, and bandwidth limiting stages, respectively.

The overall frequency response measured at the output of the photoreceiver module is shown in Fig. 5. The lower -3 dB is due to the frequency response of the bias tee which has a flat response starting 5 MHz and a minimum frequency at 100 kHz. The upper 3 dB at 6 MHz is a combination of the frequency responses of the LED and the photoreceiver module.

V. Effective SNR

Simulation results show that the OFDM signal constellations, in the presence of an LED, experience amplitude and phase distortions in a random fashion [4]. For large number of subcarriers, the OFDM signal can be accurately modeled by a Gaussian random process with a zero mean value and a variance σ_{o}^2. The probability density function (pdf) is given by:

$$P_X(x) = \frac{1}{\sqrt{2\pi\sigma_{\mathrm{o}}^2}} \exp^{-\left(\frac{x^2-\mu}{2\sigma_{\mathrm{o}}^2}\right)} \tag{1}$$

where, X is the continuous random variable which corresponds to the amplitude of the OFDM time domain samples, x denotes a sample value of X, and μ is the mean. According to the Bussgang theorem, the amplitude distortion of a Gaussian input results in a constant gain and uncorrelated additive noise [13]. Hence, by modeling this nonlinearity induced noise as Gaussian noise, a simple definition of the effective SNR, ρ, as a function of the nonlinearity induced noise power, p_{n}, is given by:

$$\begin{aligned} \rho &= \frac{\text{OFDM signal power}}{\text{Effective noise power}} \\ &= \frac{\sigma_{\mathrm{o}}^2}{\sigma_{\mathrm{AWGN}}^2 + p_{\mathrm{n}}} \end{aligned} \tag{2}$$

where, σ_{AWGN}^2 represents the shot noise and thermal noise at the optical receiver which can be modeled as AWGN [14], and p_{n} is given by:

$$p_{\mathrm{n}} = p_{\mathrm{ad}} + p_{\mathrm{uc}} + p_{\mathrm{lc}} \tag{3}$$

where, p_{ad} is the noise component due to the amplitude distortion of the OFDM signal, p_{uc} is the noise component due to the clipping/attenuation of the upper peaks of the OFDM signal, and p_{lc} is the noise component due to the clipping/attenuation of the lower peaks of the OFDM signal.

The noise component due to p_{ad} is given by:

$$p_{\mathrm{ad}} = \int_{v_l}^{v_u} (g(v_{\mathrm{LED}}) - i_{\mathrm{LED}}(v_{\mathrm{LED}}))^2 P_{V_{\mathrm{LED}}}(v_{\mathrm{LED}}) dv_{\mathrm{LED}} \tag{4}$$

where, $g(v_{\mathrm{LED}})$ is the unity slope linear curve which intersects with $i_{\mathrm{LED}}(v_{\mathrm{LED}})$, ($i_{\mathrm{LED}}$ is the current through the LED and v_{LED} is the voltage across the LED), at the chosen bias point m [15], the interval of the integral $[v_l\ v_u]$ is the interval of the amplitude distortion contribution to p_{n} in (3), and $P_{V_{\mathrm{LED}}}(v_{\mathrm{LED}})$ is the pdf of the OFDM signal given by (1) with a mean value equal to the bias point ($\mu = m$).

The noise component due to p_{uc} is given by:

$$p_{\mathrm{uc}} = \int_{v_u - m}^{\infty} (x - (v_u - m))^2 P_X(x) dx \tag{5}$$

where, $\mu = 0$ in (1). The time domain OFDM signal values above $v_u - m$ contribute to the noise component due to the clipping of the upper peaks of the OFDM signal.

The noise component due to p_{lc} is given by:

$$p_{\text{lc}} = \int_{m-v_l}^{\infty} (x - (m - v_l))^2 P_X(x) dx \tag{6}$$

where, $\mu = 0$ in (1). The time domain OFDM signal values above $m - v_l$ contribute to the noise component due to the clipping of the lower peaks of the OFDM signal.

VI. Results

Measurements are conducted in an office room to study the effect of LED nonlinear behavior on the OFDM signal. To this end, the bit-error performance of a wireless IR transmission link for different bias points and average electrical OFDM signal is considered. It should be noted that a directed line-of-sight (LOS) scenario is considered and the Tx-Rx separation distance is relatively short (40 cm), resulting from the deployment of a single LED. In addition uncoded transmission is assumed. For typical indoor distances of several meters, a transmitter module based on multiple LED array is needed to achieve the required coverage. Table I, outlines the OFDM parameters used for measurements.

TABLE I: Important OFDM parameters

OFDM parameters	
IFFT length	64
Data sub-carriers	30
CP length	2 (samples) [4]
Sampling frequency	10 (MSPS)
Modulation	4-QAM
Barker code length	13 (samples)
OFDM symbols/frame	33

The BER as a function of the bias point for different RMS OFDM signal voltages applied across the LED is shown on Fig. 6. The bias point is varied in steps of 0.1 V starting 1.3 V up to 3 V. For low bias points, it is noticed that high BER is observed. This is mainly due to the clipping of the OFDM lower peaks at the TOV and the relatively low radiant power. The BER is improved with the increase of the bias point, *i.e.* the LED is operating in a quasi-linear segment of the transfer curve, probability of clipping of the lower OFDM signal peaks is reduced, and higher radiant power corresponding to higher SNR at the receiver is obtained. The curves show a relatively flat BER performance for a certain range of bias points based on the OFDM amplitude. The range of bias points that correspond to approximately constant BER values is used to identify the optimum bias points for a specific OFDM amplitude to target a specific coverage. By further increasing the bias point, the BER starts to increase, *i.e.* the effective noise power is getting larger than the OFDM signal power.

The BER as a function of the RMS OFDM signal voltage applied across the LED for different bias points is shown on Fig. 7. Starting at 10 mV OFDM signal amplitude, the BER is improved with the increase of the OFDM signal amplitude, *i.e.* the signal power is getting larger than the effective noise power. With a further increase, the effective SNR, starts to decrease at certain amplitudes based on the bias point and consequently the BER starts to increase, *i.e.* the effective noise power is getting larger than the OFDM signal power. This is a trend that is also valid for bias points of 1.7 V and 2.0 V, but it could not be shown in the plot due to the chosen BER range. The behavior of the curve at 2.5V bias point demonstrates the BER degradation for high bias points compared to moderate bias points, *e.g.* 1.7V. The BER degradation is noticed for high RMS OFDM signal voltages as well as for low RMS signal voltages, *e.g.* 13mV, which confirms that the clipping effect is dominating p_{n} even for low RMS values (see Fig. 6).

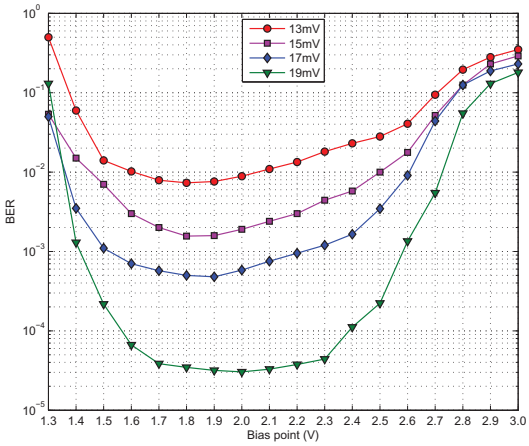

Fig. 6: The BER vs bias point. Different RMS OFDM signal voltages are considered.

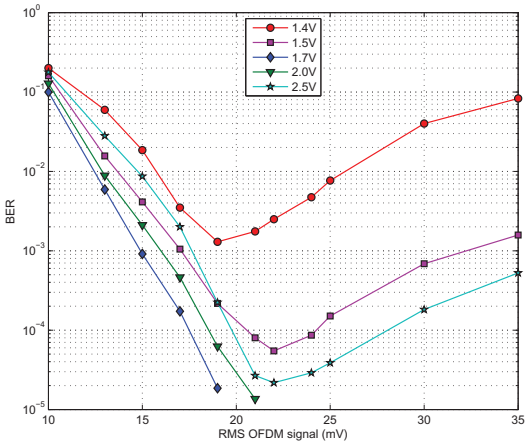

Fig. 7: The BER vs the RMS OFDM signal voltage. Different bias points are considered.

The effect of the bias point on the optical signal using a single sinusoidal carrier is highlighted in Fig. 8. The figure shows the time-domain received signal at the output of the photoreceiver module as well as the frequency domain representation (oscilloscope display). Using a bias point of 2 V, as

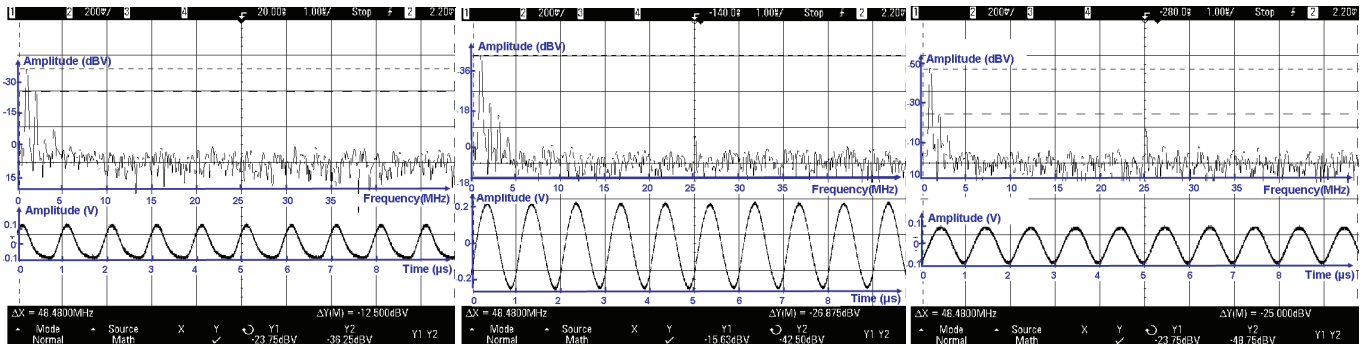

(a) (b) (c)

Fig. 8: (a) A low bias point, 1.3 V. (b) An optimum bias point, 2 V. (c) A high bias point, 3 V.

shown in Fig. 8 (b), the fundamental component is -15.63 dBV and the first harmonic shows -26.87 dBV attenuation compared to the fundamental frequency. However, for low bias point, 1.3 V, as shown on Fig. 8 (a), the lower peaks are obviously clipped, the fundamental component is -23.75 dBV, and the first harmonic shows -12.5 dBV attenuation compared to the fundamental frequency. Finally, for high bias point, 3 V, as shown on Fig. 8 (c), the signal is less distorted compared to the signal at 1.3 V bias point. The signal amplitude is attenuated compared to the signal at 2 V bias point. The fundamental component has the same amplitude as the fundamental component at 1.3 V bias point. However, the first harmonic shows -25 dBV attenuation compared to the fundamental frequency. Thus, the signal shape is also preserved for higher bias points, which explains the flat BER behavior for a certain range of bias points, *e.g.* 1.7 - 2.3 V, above the 1.5 V operation point, *i.e.* the recommended IR operation point according to the data sheet.

VII. Conclusion

For optical OFDM systems based on IM, the OFDM signal is highly distorted due to the nonlinear behavior of LEDs. An experimental setup is used to measure the BER performance using off-the-shelf components. It was demonstrated that increasing the OFDM signal amplitude modulating the LED does not necessarily mean performance enhancement. The BER is shown to be considerably improved by a proper setting of the LED operating point. For low bias currents, the OFDM signal lower peaks are clipped, which leads to a poor BER performance. However, the signal shape is preserved for a certain range of the bias currents above the recommended values for the IR LED operation which results in an improved BER performance.

Acknowledgement

We gratefully acknowledge the support for this work from EADS Germany and Airbus Germany. In addition, we acknowledge the support from the German Federal Ministry of Economics and Technology (BMWi) under grant 20K0806G as part of the Lufo 2nd Call project SINTEG.

References

[1] J. Grubor, S. Randel, K. Langer, and J. Walewski, "Bandwidth Efficient Indoor Optical Wireless Communications with White Light Emitting Diodes," in *In the Proceeding of the 6th International Symposium on Communication Systems, Networks and Digital Signal Processing*, vol. 1, Graz, Austria, Jun. 23–25, 2008, pp. 165–169.

[2] M. Z. Afgani, H. Haas, H. Elgala, and D. Knipp, "Visible Light Communication Using OFDM," in *Proc. of the 2nd International Conference on Testbeds and Research Infrastructures for the Development of Networks and Communities (TRIDENTCOM)*. Barcelona, Spain: IEEE, Mar. 1–3 2006, pp. 129–134.

[3] J. Armstrong and A. Lowery, "Power Efficient Optical OFDM," *Electronics Letters*, vol. 42, no. 6, pp. 370–372, Mar. 16, 2006.

[4] H. Elgala, R. Mesleh, and H. Haas, "Practical Considerations for Indoor Wireless Optical System Implementation using OFDM," in *Proc. of the IEEE 10th International Conference on Telecommunications (ConTel)*, Zagreb, Croatia, Jun. 8–10 2009.

[5] Y. Li and G. Stüber, Eds., *Orthogonal Frequency Division Multiplexing for Wireless Communications*. Springer, 2006.

[6] I. Neokosmidis, T. Kamalakis, J. W. Walewski, B. Inan, and T. Sphicopoulos, "Impact of Nonlinear LED Transfer Function on Discrete Multitone Modulation: Analytical Approach," *Lightwave Technology*, vol. 27, no. 22, pp. 4970–4978, 2009.

[7] B. Inan, S.C.J. Lee, S. Randel, I. Neokosmidis, A.M.J. Koonen and J.W. Walewski, "Impact of LED Nonlinearity on Discrete Multitone Modulation," *IEEE/OSA Journal of Optical Communications and Networking*, vol. 1, no. 5, pp. 439 –451, oct 2009.

[8] E. Schubert, *Light-Emitting Diodes*, 1st ed. Cambridge University Press, 2003, ISBN 0 521 82330 7.

[9] Y. Tanaka, T. Komine, S. Haruyama, and M. Nakagawa, "Indoor Visible Light Data Transmission System Utilizing White LED Lights," *IEICE Transactions on Communications*, vol. E86-B, no. 8, pp. 2440–2454, Aug. 2003.

[10] H. Elgala, R. Mesleh, H. Haas, and B. Pricope, "OFDM Visible Light Wireless Communication Based on White LEDs," in *Proc. of the 64th IEEE Vehicular Technology Conference (VTC)*, Dublin, Ireland, Apr. 22–25, 2007.

[11] A. A. Eyadeh, "Performance of Frame Synchronization Symbols for an OFDM-based Wireless Data Communication System," in *In the Proceeding of the 7th WSEAS International Conference on Data networks, Communications, Computers (DNCOCO 08)*. Bucharest, Romania: World Scientific and Engineering Academy and Society (WSEAS), Nov. 7–9, 2008, pp. 41–45.

[12] Altera Corporation, "Development kit Stratix II Edition DK-DSP-2S60N," Retrieved from http://www.altera.com, Mar. 2008.

[13] J. Bussgang, "Cross Correlation Function of Amplitude-Distorted Gaussian Signals," Research Laboratory for Electronics, Massachusetts Institute of Technology, Cambridge, MA, Technical Report 216, Mar. 1952.

[14] J. B. Carruthers and J. M. Kahn, "Modeling of Nondirected Wireless Infrared Channels," in *In the Proceeding of the IEEE Conference on Communications.: Converging Technologies for Tomorrow's Applications*, vol. 2, Dallas, TX, USA, Jun. 23–27, 1996, pp. 1227–1231.

[15] H. Elgala, R. Mesleh, and H. Haas, "Impact of LED nonlinearities on optical wireless OFDM systems," in *2010 IEEE 21st International Symposium on Personal Indoor and Mobile Radio Communications (PIMRC)*, sept 2010, pp. 634 – 638.